# Aging and Non-Linear Glassy Dynamics in a Mean-Field Model

FabriceThalmann*,†
** LEPES-CNRS, Laboratoire associé à l'UJF-Grenoble*
*BP166X 25 avenue des Martyrs 38042 Grenoble Cedex France*
*and*
*† Department of Physics and Astronomy, University of Manchester*
*Oxford Road, Manchester M13 9PL U.K.*
(May $5^{th}$, 2000)

The mean-field approach of glassy dynamics successfully describes systems which are out-of-equilibrium in their low temperature phase. In some cases an aging behaviour is found, with no stationary regime ever reached. In the presence of dissipative forces however, the dynamics is indeed stationary, but still out-of-equilibrium, as inferred by a significant violation of the fluctuation dissipation theorem. The mean-field dynamics of a particle in a random but short-range correlated environment, offers the opportunity of observing both the aging and driven stationary regimes. Using a geometrical approach previously introduced by the author, we study here the relation between these two situations, in the pure relaxational limit, *i.e.* the zero temperature case. In the stationary regime, the velocity ($v$)- force ($F$) characteristics is a power law $v \sim F^4$, while the characteristic times scale like powers of $v$, in agreement with an early proposal by Horner. The cross-over between the aging, linear-response regime and the non-linear stationary regime is smooth, and we propose a parametrisation of the correlation functions valid in both cases, by means of an "effective time". We conclude that aging and non-linear response are dual manifestations of a single out-of-equilibrium state, which might be a generic situation.

PACS numbers : 05.70.Ln, 64.70.Pf, 75.10.Nr, 83.50.Gd

## I. INTRODUCTION

Thermal equilibrium is the situation where all fast processes have already taken place while slow processes have not yet started happening [1]. At the opposite, systems with slow dynamics are characterised by a broad distribution of relaxation times, ranging from the microscopic scale ($10^{-12}$ s) to the macroscopic one (hours or days). For instance, glassy systems have an equilibration time, either infinite, or much longer than the laboratory time scale. These systems reveal their out-of-equilibrium state in phenomena like *aging* or *non-linear response*.

In these systems, the microscopic time scale is not the only relevant one, and much slower processes also take place. The slow dynamics is generally attributed to the presence of thermally activated barrier crossing in the configuration space, but others mechanisms, such as the so-called "entropic barriers" may also contribute [2]. Glassy dynamics is observed when the relaxation time $\tau$ becomes larger than the laboratory typical time scale, as it is the case for supercooled liquids [3].

The aging behaviour of spin glasses has been thoroughly investigated [4]. The thermoremanent magnetization of field cooled samples shows a strong waiting-time dependence (where the waiting-time $t_w$ is the time interval between the temperature quench and the measurement). These systems have an *a-priori* infinite internal relaxation time, and the late stage of the relaxation is instead controlled by the waiting-time itself. Moreover, field cooled (waiting for $t_w$ and switching off the field) and zero field cooled (waiting for $t_w$ and switching on the field) show a remarkable complementarity of the magnetization curves [5,6]. While out-of-equilibrium, as indicated by its significant waiting-time dependence, the response of the system is linear in the applied field, provided this one is weak enough.

Glassy dynamics is also observed in the dissipative dynamics of high-Tc superconductors. Supraconducting samples with quenched disorder, at magnetic field and temperature large enough, offer a significant resistance to a flowing dc current, due to the thermal motion of the flux lines. A transition line is believed to separate an ohmic regime (the vortex liquid) from a true superconducting state (the vortex glass) [7]. In the latter, and in the limit of a vanishingly small current $j$, the dissipation occurs by activation of "bundles" of flux lines over pinning energy barriers. According to the scaling theory of the vortex glass, the typical time needed for such a move, $\tau(j)$, diverges exponentially fast as $j$ tend to zero [8]. In this situation, the response (the voltage) is a non-linear function of the driving force (the current). The system is out-of-equilibrium, because of a constant rate dissipation, but stationary, at variance with the spin glass aging. The relaxation time $\tau(j)$ which would be infinite in the absence of driving force, is regularized by any small but constant $j$, and inversely related to the magnitude of $j$.

Important and related issues are the supercooled liquids dynamics and the rheology of soft glassy materials. In the first case, the mode-coupling approach predicts an increase of the structural relaxation time $\tau$ upon cooling [9]. Aging have been found during the early stage of molecular dynamics studies of the Lennard-Jones fluid [10,11]. On the other hand, a constant shear rate flow seems to be able to change the value of $\tau$, resulting in a shear rate dependent viscosity, *e.g.* a non-linear response of the fluid [12]. More generally, this shear-thinning behaviour is well known in the context of soft-matter rheology, and a phenomenological treatment of this phenomenon based upon glassy dynamics has been proposed [13,14]. These are situations where aging and non-linear response certainly coexist as manifestations of a more general glassy dynamics.

Among the existing theoretical approaches on glassy systems, the mean-field dynamics is a very promising one. It was already used to suggest that the presence of dissipative forces generically prevents the aging phenomenon [15,16]. In this framework, the out-of-equilibrium character of a system is made precise by the existence of a generalised fluctuation dissipation theorem, related in turn to the entropy creation rate [17].

A model of particular interest is the mean-field dynamics of a particle with a quenched pinning potential. Isolated, the particle presents an aging behaviour with a logarithmic growth of the time correlation functions [18,19]. In the presence of a time-independent driving force, the dynamics is believed to be stationary, with a power law dependence of the particle's velocity in the applied force [20].

Recently, the author presented a geometrical description of the aging and linear response regime of this model, at zero temperature [21]. This approach is extended, in this paper, to the non-linear stationary regime. As a result, we find that aging, linear response dynamics on the one hand, and stationary, non-linear response dynamics on the other hand, are indeed dual manifestations of a single out-of-equilibrium state. The constant force is found to interrupt efficiently the aging relaxational dynamics, and to control the characteristic times, which in turn control the effective friction coefficient in the stationary regime. The resulting velocity-force characteristics is $v \propto F^4$, while the cross-over time between aging and stationary regime is $t_F \propto F^{-3}$. These predictions are confronted to the numerical integration of the mean-field equations. We finally suggest a scaling behaviour for the correlation function of this model which, according to our numerical findings, interpolate smoothly between the two different regimes, demonstrating their common origin.

## II. MEAN FIELD EQUATIONS AND THE HORNER RESULT

We focus on the zero temperature relaxational dynamics of a particle in a quenched random gaussian potential [21]. The particle evolves in a $N$-dimensional space, under the simultaneous effect of a pinning force $-\boldsymbol{\nabla} V$ and a constant force $\mathcal{F}$, and the equation of motion for the vector position $\mathbf{x}(t)$ is :

$$\dot{\mathbf{x}}(t) = -\boldsymbol{\nabla} V(\mathbf{x}(t)) + \mathcal{F}. \tag{2.1}$$

The potential $V(\mathbf{x})$ is a quenched disorder, chosen from a gaussian distribution, with correlations (the overline stands for the average over the quenched disorder) :

$$\overline{V(\mathbf{x}) \cdot V(\mathbf{x}')} = N \cdot \exp\left(-\frac{\|\mathbf{x}-\mathbf{x}'\|^2}{N}\right) \ ; \ \overline{V(\mathbf{x})} = 0. \tag{2.2}$$

This form ensures a meaningful $N \to \infty$ limit, in which each coordinate $\mathbf{x}_i(t)$, or gradient component $\partial_i V(\mathbf{x})$, remains of order one, while the norms $\|\mathbf{x}(t)\|$, $\|\boldsymbol{\nabla} V\|$ scale like $N^{1/2}$. The force is directed along the direction 1.

The thermodynamic limit $N \to \infty$ is taken first, which makes the zero temperature dynamics non trivial [22]. In this mean-field limit, the relaxation process is completely described by the displacement $u$, the response function $r$ and the correlation functions $b$ and $d$, $i\tilde{x}$ being the Martin-Siggia-Rose auxiliary time [23,24].

$$u(t) = N^{-1/2}\ \overline{x_1(t)}; \tag{2.3}$$

$$r(t,t') = N^{-1} \sum_{j=1}^{N} \overline{x_j(t) \cdot i\tilde{x}_j(t')}; \tag{2.4}$$

$$b(t,t') = N^{-1} \sum_{j=2}^{N} \overline{(x_j(t) - x_j(t'))^2}; \tag{2.5}$$

$$\begin{aligned} d(t,t') &= N^{-1} \sum_{j=1}^{N} \overline{(x_j(t) - x_j(t'))^2}; \\ &= b(t,t') + [u(t) - u(t')]^2. \end{aligned} \tag{2.6}$$

The Dyson equations for $r, b, d, u$ are a closed system of coupled integro-differential equations, which contains the equations of [19,20] as a particular case :

$$\partial_t r(t,t') = \delta(t-t') \\ -4\int_0^t \mathrm{d}s\ \exp(-d(t,s))\ r(t,s)\ [r(t,t') - r(s,t')]; \tag{2.7}$$

$$\partial_t b(t,t') = (2T) - 4\int_0^t \mathrm{d}s\ \exp(-d(t,s))\ [r(t,s) - r(t',s)] \\ -4\int_0^t \mathrm{d}s\ \exp(-d(t,s))\ r(t,s)\ [b(t,s) + b(t,t') - b(s,t')]; \tag{2.8}$$

$$\partial_t u(t) = F - 4\int_0^t \mathrm{d}s\ \exp(-d(t,s))\ r(t,s)\cdot[u(t) - u(s)]. \tag{2.9}$$

The temperature term $(2T)$ is actually zero in our case. It is also convenient to define the integrated response $\mathcal{R}$ and the energy $\mathcal{E}$:

$$\mathcal{R}(t,t') = \int_{t'}^t \mathrm{d}s\ r(t,s); \tag{2.10}$$

$$\mathcal{E}(t) = -2\int_0^t \mathrm{d}s\ \exp(-d(t,s))r(t,s). \tag{2.11}$$

In a seminal paper, Horner described the stationary state reached by the system when driven with a finite force $F$, in the case of short range, power-law correlations [20]. We have found that the system (2.9) does indeed lead to a stationary situation, that we study in detail in this paper. One must mention however that the stationary state reached by the particle depends on how the system is prepared, in the same way as thermalised initial conditions can prevent aging in the $p$-spin case [25]. The stationary state is found only if the system is quenched from a high enough temperature [26]. Results for a similar driven system have also been recently published [27].

Let us summarise the main properties of the stationary solution found by Horner [20]. The correlation functions are time-translationally invariant (TTI) : $r(t,t') = R(t-t')$, $B(t,t') = B(t-t')$ while the displacement goes linearly with time $u(t) = v\cdot t$. The system (2.9) becomes a set of non-causal equations to be solved self-consistently. A non trivial feature of this solution is the emergence of characteristic time scales dependent on the velocity. With the notations of [20], $t_p(v)$ is the characteristic time for breaking the fluctuation dissipation theorem, while $t_a(v)$ controls the main "$\alpha$" relaxation of the correlation function $B(t)$. These characteristic times play a very similar role than the time scales $t_f$ and $t_b$ respectively, introduced in [21], and we identify subsequently $t_f \equiv t_p$, $t_b \equiv t_a$. In the long time regime, $t \sim t_b$:

$$B(t) = q + \hat{B}\left(\frac{t}{t_b(v)}\right), \tag{2.12}$$

with,

$$t_f(v) \sim v^{(\eta-1)\zeta}, \tag{2.13}$$

$$t_b(v) \sim v^{\eta-1},\ 0 < \eta, \zeta < 1. \tag{2.14}$$

The exponents depend (in a complex way) on the correlator (2.2) [20]. $\hat{B}$ is a scaling function discussed in appendix B, and $q$ is the "plateau value" of $B(t)$, equal to 0 in the zero temperature limit. Meanwhile, the fluctuation dissipation theorem, obeyed for $t \leq t_f$, is violated around $t \simeq t_f$, and becomes :

$$\mathrm{d}B(t)/\mathrm{d}t = 2\overline{T}R(t);\ t \gg t_f. \tag{2.15}$$

The effective temperature $\overline{T}$ and the plateau value $q$ are identical to those obtained in the aging case [19].

The velocity-force characteristics is given by (2.9), and in the limit of small velocities,

$$v \sim F/t_b(v). \tag{2.16}$$

The time $t_b(v)$ plays the role of an effective friction coefficient, controlled by the velocity. The $v - F$ characteristics is a power law.

$$v \sim F^{1/\eta}. \tag{2.17}$$

Let us mention for completeness the presence of a third time scale, called $t'_a$ in [20], defined by $B(t'_a) = v^2 t'^2_a$. As we consider an exponential correlator, we have $\exp(-B(t) - v^2t^2) \equiv \exp(-B(t)) \times \exp(-v^2t^2)$ and in our case $t'_a \sim v^{-1}$. We believe that apart from this point, the results of [20] all qualitatively apply to the exponential correlator, and anyway $t'_a$ does not play a direct role in the dynamics of the short range correlated models.

## III. GEOMETRICAL DESCRIPTION OF THE DRIVEN STATIONARY DYNAMICS

In [21] was proposed a geometrical description of the relaxational dynamics of the particle. This approach makes use of a comoving frame, defined by the eigendirections of the hessian matrix $\boldsymbol{\nabla}\boldsymbol{\nabla}V(\mathbf{x})$ at the precise point $\mathbf{x}(t)$ where the particle stands. This frame is made of $N$ vectors $\{\mathbf{e}_i\}$, each one eigenvector of the hessian $\boldsymbol{\nabla}\boldsymbol{\nabla}V(\mathbf{x})$. The distribution of the corresponding eigenvalues is a semi-circle of radius 4, shifted towards the positive values, and such that the lowest one is equal to $-\mathcal{S}$. Each eigenvector $\mathbf{e}_i$ has an eigenvalue $\lambda_i - \mathcal{S}$, and the density of states of the $\lambda_i$ is :

$$\rho(\lambda) = (8\pi)^{-1}\sqrt{\lambda\ (8-\lambda)}. \tag{3.1}$$

The quantity $\mathcal{S}$ is positive, and depends linearly on the energy of the system, *e.g.* $\mathcal{S}(t) = 4 + 2V(\mathbf{x}(t))/N = 4 + 2\mathcal{E}(t)$. In the aging case, $\mathcal{S}(t)$ is a time-dependent function, while in the stationary case, $\mathcal{S}$ is constant.

One projects the instantaneous velocity $\dot{\mathbf{x}}$ is the above frame such that:

$$\dot{\mathbf{x}} = \sum_{i=1}^{N} \gamma_i \mathbf{e}_i \tag{3.2}$$

Because the spacing of the eigenvalues is of order $1/N$, the set of $\lambda_i$ becomes dense, and one replaces the discrete sum over the index $i$ by a continuous one, involving the semi-circular density of eigenvalues $\rho(\lambda)$.

$$\dot{\mathbf{x}}^2 = \int_0^8 \mathrm{d}\lambda\ \rho(\lambda)\ g(\lambda, t) \tag{3.3}$$

The distribution $g(\lambda, t)$ represents the mean value of the component $\mathbf{x}_i^2$, locally averaged over the indices $i$ such that $\lambda_i \simeq \lambda$. We have justified in [21] the following self-similar form for $g(\lambda, t)$:

$$\begin{aligned} \mathbf{x}_i^2 &\sim g(\lambda_i, t) \\ g(\lambda, t) &= \mathcal{S}(t)\hat{G}\Big(\lambda/\mathcal{S}(t)\Big), \end{aligned} \tag{3.4}$$

where $\lambda$ stands for any direction with a curvature of the potential equal to $\lambda - \mathcal{S}$ [21]. The prefactor $\mathcal{S}$ in front of the distribution comes in fact from an assumption about the value of the exponent $-\kappa$ governing the power law decay of $\mathcal{E}(t)$ and $\mathcal{S}(t) \sim t^{-\kappa}$, which we believe to be $-2/3$. This assumption is supported by our numerical results.

The characteristic times $t_f$ and $t_b$ are controlled by $\mathcal{S}$, and scale like :

$$\begin{aligned} t_f &\sim \mathcal{S}^{-1}; \\ t_b &\sim \mathcal{S}^{-3/2}; \end{aligned} \tag{3.5}$$

making the instantaneous velocity equal to :

$$\dot{u}(t) = F \cdot \mathcal{S}^{3/2} = F/t_b(t). \tag{3.6}$$

When a constant force $F$ is applied, the dynamics changes from an aging linear-response behaviour to a stationary regime [21]. At short times, the displacement $u(t)$ is proportional to the integrated response $F \cdot \mathcal{R}(t, 0)$, while at long times, it becomes equal to $v \cdot t$.

One expects the stationary regime to take over the aging regime when the dynamics is dominated by the external force $\mathcal{F}$ rather than by the gradient $-\boldsymbol{\nabla}V(\mathbf{x}(t))$. This happens at a time $t_F$, inversely related to the magnitude of the force. Our numerical definition of $t_F$, is the time where the slope of the asymptotic curve $u(t)/F \simeq vt/F$ is equal to the slope of the (logarithmic) integrated response $\mathcal{R}(t, 0)$, as shown on Figure (1) with $F = 0.3$.

In our situation, the dynamics is controlled by the value of $\mathcal{S}$; inverse friction and diffusion coefficients are both proportional to $\mathcal{S}^{3/2}$. In the aging case, $\mathcal{S}(t)$ tends to zero as a power law, and the dynamics of the system is slower and slower. A look at Figure (2) however shows that in the presence of a force, $\mathcal{S}$ does not go to zero, but to a finite value $\mathcal{S}(F)$, controlled by $F$, and inversely related to the magnitude of $F$. The same is true for the energy $\mathcal{E}(t) = -2 + \mathcal{S}(t)/2$, which stands higher than in the absence of driving force. Both diffusivity and mobility are kept finite thanks to a non-zero driving force. What is needed is to compute $\mathcal{S}(F)$. For this purpose, one assumes that the self-similar form (3.4) is still valid in the stationary regime. A justification is provided in appendix A.

The zero temperature relaxation equation is:

$$\dot{\mathbf{x}}_i = -\partial_i V(\mathbf{x}) + \mathcal{F}_i, \tag{3.7}$$

while the energy obeys :

$$\dot{\mathcal{E}}(t) = 1/N \sum_i \partial_i V(\mathbf{x}(t)) \cdot \dot{\mathbf{x}}_i(t),$$
$$\dot{\mathcal{E}}(t) = -\dot{\mathbf{x}}^2(t)/N + F \cdot \dot{u}(t). \tag{3.8}$$

One uses now the distribution $g(\lambda, t)$ of the instantaneous velocity components $\dot{\mathbf{x}}_i^2$, the density of eigenvalues $\rho(\lambda)$ and finds :

$$-\dot{\mathcal{E}}(t) + F \cdot \dot{u}(t) = \int \mathrm{d}\lambda \ \rho(\lambda) \ g(\lambda, t). \tag{3.9}$$

In the stationary regime, $\dot{\mathcal{E}}(t) = 0$ and $\dot{u}(t) = v$. The equation (3.9) reduces to a balance between the mechanical power given by the force, and a kind of intrinsic dissipation ($\dot{\mathbf{x}}^2$).

$$F \cdot v = \int \mathrm{d}\lambda \ \rho(\lambda) \ g(\lambda). \tag{3.10}$$

Assuming that $g$ is still equal to $\mathcal{S}\hat{G}(\lambda/\mathcal{S})$ (cf appendix A), one gets :

$$F \cdot v \sim \mathcal{S}^{5/2}. \tag{3.11}$$

From (3.11) and (3.6), one finally finds $\mathcal{S}$ as a function of the force,

$$\mathcal{S} \sim F^2, \tag{3.12}$$

the resulting velocity force characteristics,

$$v \sim F^4, \tag{3.13}$$

and the force and velocity dependence of the time scales :

$$t_f \sim F^{-2} \sim v^{-1/2}; \tag{3.14}$$
$$t_b \sim F^{-3} \sim v^{-3/4}. \tag{3.15}$$

These results are in full qualitative agreement with the findings of Horner [20]. The main relaxation time $t_b$ does not scale as $v^{-1}$, as could be expected from a simple dimensional analysis, but is shorter, such that $\lim_{v\to 0} v \cdot t_b(v) = 0$.

One determines the cross-over time $t_F$ by a matching argument. In the linear response regime, $\mathcal{S}(t)$ decreases as $t^{-2/3}$, as the force acts only as a weak perturbation. The linear response breaks down when the perturbation modifies the nature of the relaxation itself. This happens when $\mathcal{S}(t_F)$ reaches the order of magnitude of its limit value $\mathcal{S}(F) = F^2$ (equation 3.12), leading to $t_F^{-2/3} = F^2$, or:

$$t_F = F^{-3}. \tag{3.16}$$

Physically, this means that a typical coordinate $f_i$ of the force $\mathcal{F}$, along a downhill direction $i$, is of the same order of magnitude than the gradient of the potential $-\partial_i V$ , or the instantaneous velocity $\dot{\mathbf{x}}_i$ [21]. From equation (3.4) and $f_i \simeq F$, one gets $F^2 \simeq f_i^2 \simeq \dot{\mathbf{x}}_i^2 \simeq \mathcal{S}$, in agreement with (3.12).

Let us mention that a qualitatively similar cross-over has been observed in the simulated dynamics of a driven polymer, in the presence of quenched disorder [28].

## IV. NUMERICAL RESULTS

We present numerical results which support the findings of the previous section.

Figure (3) shows $\mathcal{S}(F)$ *versus* $F$, in log coordinates, and in regular coordinates (inset), for $F = 0.05, 0.1, 0.2, 0.3, 0.4, 0.5$ and $F = 0.6$. The squares are the values obtained with $t_{max} = 200$ ($h = 0.1$), and the full curve with $t_{max} = 400$ ($h = 0.2$). One sees that the three first values are not well converged. If we except them, the overall shape of the curve is concave (downward curvature). The slope of the tangent curve between the arrows gives an exponent equal to 1.81 ($h = 0.1$) and 1.87 ($h = 0.2$). Because the curve is concave, we believe that these values are a lower bound for the real exponent, compatible with our prediction 2.

Figure (4) shows $v(F)$ *versus* $F$, in log coordinates, and in regular coordinates (inset). The squares are the values obtained with $t_{max} = 200$ ($h = 0.1$), and the crosses with $t_{max} = 400$ ($h = 0.2$). As for Figure (3), the three first values are not well converged. If we except them, the overall shape of the curve is again concave. The slope of the tangent curve between the arrows gives an exponent equal to 3.73 ($h = 0.1$) and 3.82 ($h = 0.2$). Repeating the above argument, these values are a lower bound for the real exponent, compatible with 4.

A plot of $t_F$ *vs* $F$ is reported on Figure (5). Again the system has not reached its asymptotic regime as far as the three first values $F \leq 0.2$ are concerned. This can be checked by looking at the first derivative $\dot{u}(t)$ which must be constant when $t$ reaches the upper limit of the time window, here $t = 400$. The fitted value on the straight part of the graph, in logarithmic coordinates, gives an exponent $-2.72$ instead of $-3$. Again the true asymptotic limit $F \to 0$ is out of reach, due to our limited computer facilities.

These numerical results are not good enough to prove the exactness of the equations (3.12) and (3.13). However they provide lower bounds which constraint the exponents to be larger than 1.8 for $\mathcal{S}$, and larger than 3.8 for $v$. On the other hand, if we assume that we are close enough to the asymptotic regime where equations (3.12) and (3.13) apply, one expects the real exponents to be not too much different from the above numerical values. In this respect, we think that the numerics is in agreement with our findings. As far as the cross-over time is concerned, the numerical exponent is $-2.72$ instead of $-3$. A larger time window would certainly improve the agreement.

## V. A UNIFIED DESCRIPTION OF THE OUT-OF-EQUILIBRIUM REGIMES

In the isolated aging regime, at zero temperature, the correlation function obeys, as a particular case of equation (B1) of appendix B, as shown in [19] :

$$b(t, t') = \ln\left(\frac{h(t)}{h(t')}\right), \tag{5.1}$$

where the parametrisation function is related to the time-scale $t_b$ by :

$$t_b(t) = h(t)/h'(t) \tag{5.2}$$

As the time scale $t_b$ is proportional to $\mathcal{S}^{-3/2}$, we have :

$$\frac{h(t)}{h(t')} = \exp\left[C \int_{t'}^{t} \mathrm{d}s\ \mathcal{S}^{3/2}\right],$$
$$b(t, t') = C \int_{t'}^{t} \mathrm{d}s\ \mathcal{S}^{3/2}. \tag{5.3}$$

On the other hand, equation (3.6) leads immediately to

$$\frac{u(t) - u(t')}{F} = C' \int_{t'}^{t} \mathrm{d}s\ \mathcal{S}^{3/2}. \tag{5.4}$$

Now, one observes that the scaling form (2.12) resemble to (5.1), (B1), with $q = 0$. We prove in appendix B that the scaling function of the aging regime [19] and the driven regime [20] are indeed equal, and thus $\hat{B}(x) = x$ in (2.12) (strictly speaking, $\hat{B}(x)$ is only proportional to $x$, but one can choose $t_b$ such as $\hat{B}(x) = x$). The equations (5.3) and (5.4) make sense in the aging regime as well as in the stationary regime.

The integral $\int_{t'}^{t} \mathrm{d}s\ \mathcal{S}^{3/2}$ is the *effective time* variable for the system, interpolating smoothly between $\ln(t)$ (aging, linear response regime) and $t/t_b(F)$ (stationary regime) while $S^{-3/2}$ is an *effective age*, growing like the waiting time,

in the aging regime, and bounded in the stationary regime. Interestingly, a similar effective age has been used in the context of the stick-slip motion in dry friction experiments [29].

The prediction for (5.3) and (5.4) is checked by plotting $b(t,t')$ vs $[u(t)-u(t')]/F$, shown on Figures (6) and (7). One expects $b(t,t')$ and $[u(t)-u(t')]/F$ to be proportional, both in the aging and stationary regimes, provided equations (5.3, 5.4) hold, which is the case for a time separation $t-t'$ large enough.

On Figure (6), $b(t,t')$ is plotted against $[u(t)-u(t')]/F$ for $F=0.1$ (crosses, squares and diamonds) in the linear response regime and for $F=0.5$ (continuous lines) in the non-linear regime. The force is zero till $t=t'$, and then switched on; $t'$ takes the value 0, 20 and 40. As far as $F=0.5$ is concerned, the transition from linear to non-linear regime is not visible on this curve, and in any case very smooth. The slope of the curve defines the effective temperature $2\overline{T}$, equal to the ratio $C/C'$ in equations (5.3) and (5.4). The effective temperature thus makes sense in both linear and non-linear regimes.

As the force is switched on at $t'$, there is a short-time "elastic" displacement. This is how the directions with a positive curvature respond to the new static constraint, and this corresponds to the short horizontal step at the origin, seen on Figures (6) (inset) and (7). The finite slope part of the curve corresponds to the slow wandering motion of the particle in the energy landscape, in the regime where equations (5.3) and (5.4) apply. Thus, we conclude that Figure (6) support the proportionality of $u(t)-u(t')$ and $b(t,t')$, once the short time regime has been taken into account.

A close look near the origin of the graph (inset of Figure (6) shows that the $F=0.5$ curve is slightly shifted from $F=0.1$, but parallel to it. This shift goes rapidly to zero as $F\to 0$. The shift is presumably there because 0.5 is already a large value of the force, leading to a departure from the ideal curve corresponding to $F\ll 1$.

Figure (7) is the same as Figure (6) for $F=0.01$, $F=0.1$ and $F=0.5$, for three values of $t'$, 0, 20 and 40, and gives additional details on the short time response of the particle. Again, the horizontal part of the curves corresponds to the short-time displacement ("elastic" or reversible) while the finite slope regime corresponds to the slow motion in the energy landscape ("plastic" or irreversible).

## VI. CONCLUSION

In this paper, we have proposed a consistent picture for the stationary driven dynamics, in the mean field approximation and zero temperature limit, of a particle in a quenched, exponentially correlated, random potential.

The velocity ($v$)- force ($F$) relation is a power law $v=F^4$, while the main relaxation time scales as $t_b \simeq v^{-3/4}$. The product $v\cdot t_b$ tends to zero as $v$ vanishes. These findings are consistent with earlier work [20]. The driving force is found to generate a relaxation time smaller than the "dimensional" time scale $v^{-1}$, which is probably a generic feature of the mean-field short-range correlated potentials.

If the force $F$ is small enough, a linear response around the aging regime is found, up to a time $t_F$, scaling as $F^{-3}$. A plot of the displacement $(u(t)-u(t'))/F$ *vs* the correlation $b(t,t')$ shows no sign of discontinuity, when the linear response regime is replaced with the non-linear stationary regime. We interpret it by saying that, when a small force is applied, the dynamical properties of the system (mobility, diffusivity) are controlled by the *effective age* $\mathcal{S}^{-3/2}$. The quantity $\mathcal{S}^{3/2}$ is proportional to the number of negative eigenvalues in the spectrum of the hessian of the hamiltonian. The effective age is proportional to the waiting time in the aging regime, and finite in the stationary case.

The *effective time* $\int^t \mathcal{S}^{3/2}\mathrm{d}s$, closely related to the correlation function $b(t,t_0)$, grows logarithmically with $t$ in the aging regime, and linearly with $t$ in the stationary regime. The effective temperature $\overline{T}$ generalising the fluctuation dissipation theorem, remains unchanged in the non-linear regime. However, the geometrical meaning of $\overline{T}$, if any, is still unknown.

Future work will determine to what extent are the present features generic from other short range correlated models, and finite dimensional models. Even though such a power law dependence of the characteristic times in the driving force is not observed in realistic systems, the qualitative behaviour presented in this study –cross-over between linear to non-linear regime, coexistence of aging and non-linear stationary dynamics–, could indeed be a very generic situation.

*Acknowledgements* I especially thank L.Cugliandolo and J.Kurchan for having lent me their numerical code, and S.Scheidl, J.P Bouchaud, J.Kurchan, M.Mézard and A.Cavagna for discussions on this field. I thank D.Feinberg for suggestions and criticisms about the manuscript. I warmly thank the hospitality of the Department of Physics, IISc, Bangalore, where a part of the writing has been done.

## APPENDIX A: THE ENERGY BALANCE

Let $\gamma_i(t)$ be the coordinates of the instantaneous velocity $\dot{\mathbf{x}}(t)$ in the comoving frame $\{\mathbf{e}_i(t)\}$ (3.2). When $\mathcal{F}=0$, this definition is equivalent to say that $\gamma_i$ is the coordinate of $-\boldsymbol{\nabla}V$. Using the local average defined in [21], one finds:

$$\begin{aligned}\|\dot{\mathbf{x}}\|^2(t) &= \sum_i \dot{\mathbf{x}}_i^2(t) = \sum_i \gamma_i^2(t),\\ &= N\int \mathrm{d}\lambda\ \rho(\lambda)\ g(\lambda,t).\end{aligned} \tag{A1}$$

The derivative of $\|\dot{\mathbf{x}}\|^2(t)$ reads :

$$\begin{aligned}\partial_t\|\dot{\mathbf{x}}\|^2(t) &= \sum_j^N \partial_t(-\partial_j V+\mathcal{F}_j)^2\\ &= -2\sum_{jk}\partial_{jk}V\cdot\dot{\mathbf{x}}_j\cdot\dot{\mathbf{x}}_k\\ &= -2N\int \mathrm{d}\lambda\ \rho(\lambda)\ (\lambda-\mathcal{S})\cdot g(\lambda,t).\end{aligned} \tag{A2}$$

We deduce that, in the stationary situation, for all $\mathcal{S}$,

$$\int \mathrm{d}\lambda\ \rho(\lambda)\ \lambda\ g(\lambda) = \mathcal{S}\int \mathrm{d}\lambda\ \rho(\lambda)\ g(\lambda), \tag{A3}$$

which is in favour of a scaling form $g(\lambda)=\Gamma\hat{G}(\lambda/\mathcal{S})$.

As $\partial_i V(\mathbf{x}(t)) = -\dot{\mathbf{x}}_i(t)+\mathcal{F}_i$, the equation for $\dot{\mathcal{E}}(t)$ is :

$$\begin{aligned}\dot{\mathcal{E}}(t) &= N^{-1}\sum_j \partial_j V\cdot\dot{\mathbf{x}}_j\\ &= N^{-1}\sum_j\{-\dot{\mathbf{x}}_j^2(t)+\mathcal{F}_j\cdot\dot{\mathbf{x}}_j(t)\}\end{aligned}$$

The product $N^{-1}\sum_j \mathcal{F}_j\cdot\dot{\mathbf{x}}_j$ is by construction equal to $F\cdot\dot{u}(t)$. Thus, (this is equation 3.9):

$$\dot{\mathcal{E}}(t) = -\int \mathrm{d}\lambda\ \rho(\lambda)\ g(\lambda,t) + F\cdot\dot{u}(t). \tag{A4}$$

The energy balance (3.11), and the factorised form of $g(\lambda)$ imply in the stationary regime :

$$\Gamma\cdot\mathcal{S}^{3/2}\propto F^2\cdot\mathcal{S}^{3/2} \tag{A5}$$

However the relation between $\mathcal{S}$ and $\Gamma$ remains undetermined by the present argument. For the sake of simplicity, we can suppose that the equality $\mathcal{S}=\Gamma$, true in the aging regime, remains true in the stationary regime. This assumption is in fact equivalent to a matching argument, when the distribution $g(\lambda,t)=\mathcal{S}(t)\hat{G}(\lambda/\mathcal{S}(t))$, crosses over the distribution $g(\lambda)=F^2\hat{G}(\lambda/\mathcal{S}(F))$ around $t=t_F$. The matching of $g(\lambda,t)$ and $g(\lambda)$ leads to the identification $\mathcal{S}(F)=F^2$. One cannot rule out, rigorously, more complicated behaviours, which could lead to a different velocity-force characteristics. The assumption $\Gamma=\mathcal{S}$ is just the most natural one.

## APPENDIX B: THE SCALING FORM OF THE CORRELATION FUNCTION

In the isolated situation, the correlation function in the aging regime reads, for any finite temperature $T$ [19,30]:

$$b(t,t') = q+\tilde{B}\left[\ln\left(\frac{h(t)}{h(t')}\right)\right] \tag{B1}$$

An general equation for $\tilde{B}(u)$ is obtained in reference [19] (equation 6.22, with the opposite sign convention for $f$), and reads:

$$0 = \tilde{B}(u)f''(q) - f'(q+\tilde{B}(u)) + f'(q) + \frac{2\chi q}{T} f''(q) \int_0^u \mathrm{d}u' \ \tilde{B}'(u') f''(q+\tilde{B}(u))\tilde{B}(u-u') \tag{B2}$$

whose solution is $\tilde{B}(u) = C^{st} \times u$, leading to (5.1), with $q = 0$. The function $f = \exp(-x)$ stands for the correlator (2.2), $T$ for the temperature, $q$ for plateau value of the correlation function $b$, and $\chi$ for the fluctuation dissipation violation parameter (see equation B4 below).

On the other hand, in the stationary regime, the equation for $b(t,t') = B(t-t') = q + \overline{B}(t-t')$ and $R(t-t') = r(t,t')$ is (equation (2.9) in reference [20], again with the opposite sign convention for $f$):

$$\begin{aligned}\partial_t B(t) = 2T &- \left( \int_0^\infty \mathrm{d}s \ 4f''(B(s)+v^2s^2)R(s) \right) \cdot B(t) + \int_0^t \mathrm{d}s \ 4f''(B(s)+v^2s^2)R(s)B(t-s) \\ &+ \int_0^\infty \mathrm{d}s \ \Big\{ \Big( 4f'(B(t+s)+v^2(t+s)^2) - 4f'(B(s)+v^2s^2) \Big) R(s) \\ &+ \Big( 4f''(B(t+s)+v^2(t+s)^2)R(t+s) - 4f''(B(s)+v^2s^2)R(s) \Big) B(s) \Big\}\end{aligned} \tag{B3}$$

One knows that the main relaxation scale $t_b$ is much smaller than $v^{-1}$, and asymptotically, $\lim_{t\to 0} v \cdot t_b = 0$. The above integrals can be safely cut beyond a cut-off $\Lambda$ such that $t_b \ll \Lambda \ll v^{-1}$. The contributions $\int_\Lambda^\infty$ are negligible because the relaxation of $B(t)$ has already taken place, while in the integrals $\int_0^\Lambda$, the term $v^2s^2$ can be neglected compared with $B(s)$ in the argument of the correlators $f'$ and $f''$.

One introduces the quasi fluctuation dissipation parameter $X$, defined by:

$$-X(\overline{B}(t)) \cdot \mathrm{d}B(t)/\mathrm{d}t = R(t). \tag{B4}$$

$X$ is equal to its equilibrium value $-1/2T$ if $\overline{B} < 0$ and to $\chi$ if $\overline{B} > 0$. Equation (B3) becomes:

$$\begin{aligned}\partial_t B(t) = 2T &+ \left( \int_0^\Lambda \mathrm{d}s \ 4f''(q+\overline{B}(s))X(\overline{B}(s))\mathrm{d}\overline{B}(s)/\mathrm{d}s \right) B(t) - \int_0^t 4f''(\overline{B}(s))X(\overline{B}(s))\mathrm{d}\overline{B}(s)/\mathrm{d}s \ \cdot B(t-s) \\ &- \int_0^\Lambda \mathrm{d}s \ \Big\{ \Big( 4f'(q+\overline{B}(t+s)) - 4f'(q+\overline{B}(s)) \Big) X(\overline{B}(s))\mathrm{d}\overline{B}(s)/\mathrm{d}s \\ &+ \Big( 4f''(q+\overline{B}(t+s))X(\overline{B}(t+s))\mathrm{d}\overline{B}(t+s)/\mathrm{d}s - 4f''(q+\overline{B}(s))X(\overline{B}(s))\mathrm{d}\overline{B}(s)/\mathrm{d}s \Big) \Big\} B(t)\end{aligned} \tag{B5}$$

Each integral $\int_a^b$ has to be split to take into account the short time quasi-equilibrium regime and the long time regime. As the time scale $t_f$ separates these two regimes, one writes $\int_a^b = \int_a^{a+t_f} + \int_{a+t_f}^{b-t_f} + \int_{b-t_f}^b$. The parameter $X$ is then set to $-1/2T$ or $\chi$ accordingly, and most of the integrals can be reduced to boundary terms. One neglects the time derivative $\partial_t B(t)$ in the asymptotic long-time regime, and the result is:

$$\begin{aligned}0 = 2T &+ \left( 4\chi \int_{t_f \simeq 0}^{\Lambda \simeq \infty} f''(q+\overline{B})\mathrm{d}\overline{B} \right) (q+\overline{B}(t)) \\ &- 4q \left( \chi + \frac{1}{2T} \right) \times \Big( f'(q) - f'(q+\overline{B}(t)) \Big) \\ &- 4\chi \int_{t_f \simeq 0}^t \mathrm{d}s \ \mathrm{d}\overline{B}(s)/\mathrm{d}s \ f''(q+\overline{B}(s))(q+\overline{B}(t-s))\end{aligned} \tag{B6}$$

By using $\lim_{t\to\infty} \overline{B}(t) = \infty$, $q^2 f''(q) = T^2$ and $-4\chi \int f''(\overline{B})\mathrm{d}\overline{B} = 2T/q$, the equation (B6) for $\overline{B}$ coincides exactly with (B2). As the equation (B6) is invariant upon time dilatations, $\hat{B}(u) = \overline{B}(t/t_b)$ is a solution of (B2) and without loss of generality, one has:

$$\hat{B}(u) = \tilde{B}(u) = u, \tag{B7}$$

which is the announced result.

[1] Shang-Keng Ma. *Statistical Mechanics*. World Scientific, 1985.
[2] J.P Bouchaud. *J.de Physique I(France)*, 2(9):1705, 1992. J.P Bouchaud and D.S Dean. *J.de Physique I(France)*, 5:265, 1995. S Franz and F Ritort. *J.of Physics A*, 30:L359, 1997.
[3] C.A Angell. *Science*, 267:1924, March 1995. M.G Ediger, C.A Angell, and S.R Nagel. *J.Phys.Chem.*, 100:13200, 1996.
[4] J Hammann *et al.* Comparative review of aging properties in spin glasses and other disordered materials. In *Frontiers in Magnetism, Kyoto 99*, 1999. E Vincent *et al.* Slow dynamics and aging in spin glasses. cond-mat/9607224. J.P Bouchaud, L Cugliandolo, J Kurchan, and M Mézard. Out of equilibrium dynamics in spin glasses and other glassy systems. In A.P Young, editor, *Spin Glasses and Random Fields*. World Scientific, 1997.
[5] E Vincent, J Hammann, and M Ocio. *in Slow dynamics in spin glasses and other complex systems, D.H. Ryan ed.*. World Scientific, 1992.
[6] P Nordblad, L Lundgren, and L Sandlund. *J.Magn.Magn.Mat.*, 54-57:185, 1986.
[7] M.P.A. Fisher. *Phys.Rev.Lett.*, 62:1415, 1989. D.S Fisher, M.P.A Fisher, and D.A Huse. *Phys.Rev.B*, 43:130, 1991.
[8] M.V Feigel'man, V.B Geshkenbein, L.A Larkin, and V.M Vinokur. *Phys.Rev.Letters*, 63(20):2303, 1989. G Blatter, V.B Geshkenbein, M Feigel'man, A.I Larkin, and V.M Vinokur. Vortices in high temperature superconductors. *Review of Modern Physics*, 66(4):1125, 1994.
[9] U Bengtzelius, W Götze, and A Sjölander. *J.of Physics C*, 17:5915, 1984. W Götze, in J.P Hansen, D Lesveque, and J Zinn-Justin, editors, *Liquids,freezing and glass transitions.*, Les Houches Summer School, page 289. North Holland, 1989.
[10] Giorgio Parisi. *J.of Physics A*, 30:L765, 1997.
[11] Jean-Louis Barrat and Walter Kob. *EuroPhys.Lett.*, 46(5):637, 1999.
[12] Ryoichi Yamamoto and Akira Onuki. *Phys.Rev.E*, 58(3):3515, 1998.
[13] P Sollitch, F Lequeux, P Hébraud, and M Cates. *Phys.Rev.Lett.*, 78:2020, 1997.
[14] R Evans, M Cates, and P Sollitch. *EuroPhys.J.B*, 10:705, 1999.
[15] Leticia F Cugliandolo, Jorge Kurchan, Pierre Le Doussal, and Luca Peliti. *Phys.Rev.Lett.*, 78(2):350, 350.
[16] J Kurchan. Rheology or how to stop aging. cond-mat/9812347.
[17] L Cugliandolo, D Dean, and J Kurchan. *Phys.Rev.Lett.*, 79(12):2168, 1997.
[18] S Franz and M Mézard. *Europhysics Letters*, 26(3):209, 1994. *Physica A*, 210:48, 1994.
[19] L Cugliandolo and P Le Doussal. *Phys.Rev.E*, 53(2):1525, 1996.
[20] H Horner. *Z. für physik B*, 100(2):243, 1996.
[21] Thalmann Fabrice. Geometrical approach for the mean-field dynamics of a particle in a short-range correlated random environment. Submitted to EPJB, cond-mat/0005161.
[22] J Kurchan and L Laloux. *Phys.Rev.A*, 29:1929, 1996.
[23] P Martin, E Siggia, and H Rose. *Phys.Rev.A*, 8:423, 1973.
[24] C De Dominicis. *Phys.Rev.B*, 18(9):4913, 1978.
[25] A Barrat, R Burioni, and M Mézard. *J.of Physics A*, 29:L81, 1996.
[26] Thalmann Fabrice. To be published.
[27] Ludovic Berthier, Jean-Louis Barrat, and Jorge Kurchan. Two-time scales, two temperatures scenario of non-linear rheology. cond-mat/9910305.
[28] H Yoshino. *Phys.Rev.Lett.*, 81:1493, 1998.
[29] F Heslot, T Baumberger, B Perrin, B Caroli, and C Caroli. *Phys.Rev.E*, 49:4973, 1994.
[30] L Cugliandolo and J Kurchan. *J.of Physics A*, 27:5749, 1994.

# Captions

FIGURE 1. Determination of the cross-over time $t_F$, defined as the time where the slope of the integrated response $\mathcal{R}(t,0)$ is equal to the velocity $1/F \lim_{t\to\infty} \dot{u}(t)$.

FIGURE 2. Family of curves $\mathcal{E}(t)+2$ for increasing forces, ranging from $F = 0.05$ to 0.5. The limit value $\lim_{t\to\infty} \mathcal{E}(t)+2$ is a monotonically increasing function of $F$, equal to $\mathcal{S}(F)/2$. The effective mobility and diffusivity are directly related to $\mathcal{S}(F)$. The system stays above the marginal states, in a region with a finite extensive number of downhill directions.

FIGURE 3 The parameter $\mathcal{S}$ as a function of the force, for $F = 0.1, 0.2, 0.3, 0.4, 0.5$ and 0.6, in log coordinates, and normal coordinates (inset). The boxes stand for a run, up to a time $t = 200$ while the straight line corresponds to $t = 400$. Whenever the boxes differ from the line, the value is not converged. See text for details.

FIGURE 4. The velocity $v$ as a function of the force $F$, in log coordinates, and normal coordinates (inset). Same remark as for Figure (4).

FIGURE 5. The time $t_F$ as a function of the force $F$ in log coordinates. Inset : $t_F$ as a function of $F$. The three first values are not accurate ($t_F$ larger than our maximum time). The fitted exponent of the straight part is $-2.72$ instead of 3; $-2.72$ is a lower bound for the real value.

FIGURE 6. The correlation $b(t,t')$ *vs* the displacement $[u(t)-u(t')]/F$, for $F = 0.1$ and 0.5. The force is switched on at $t'$, successively equal to $0, 20$ and 40. Inset: the short-time behaviour. See text for details.

FIGURE 7. Same as Figure (6), with $F = 0.01$, $F = 0.1$ and $F = 0.5$.

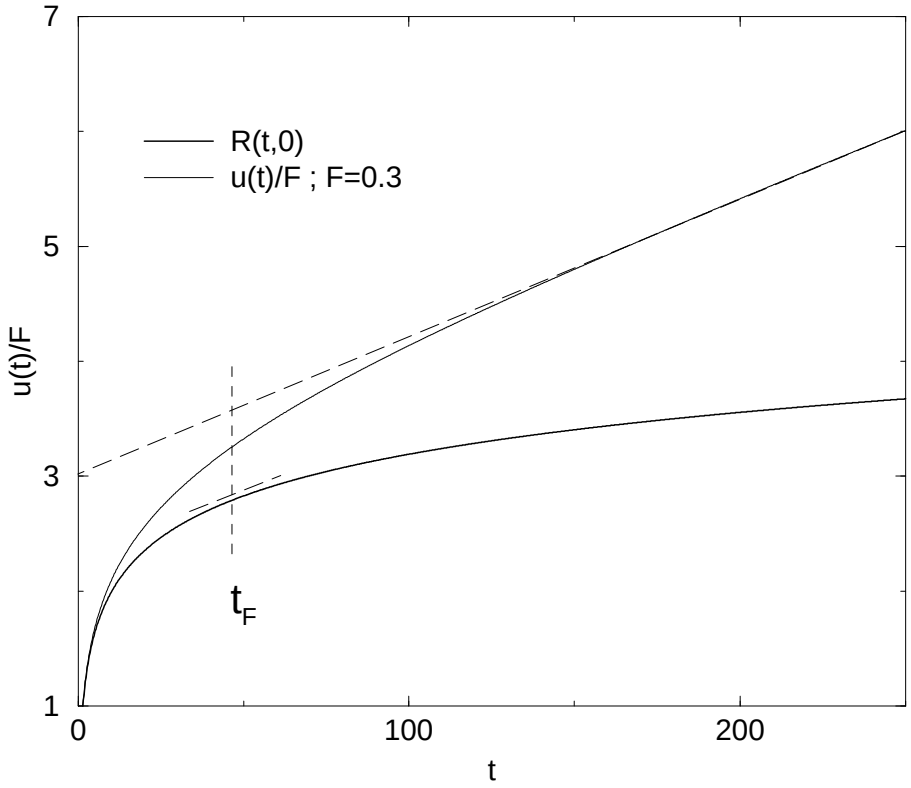
R(t,0)
u(t)/F ; F=0.3
u(t)/F
t
$t_F$
7
5
3
1
0
100
200

FIG. 1.

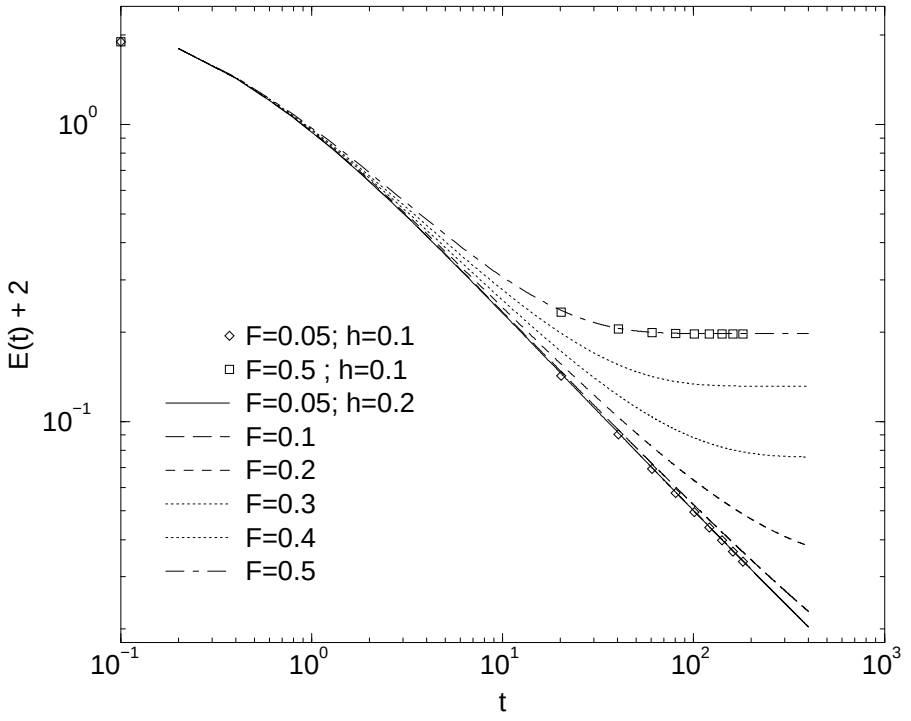
F=0.05; h=0.1
F=0.5 ; h=0.1
F=0.05; h=0.2
F=0.1
F=0.2
F=0.3
F=0.4
F=0.5
E(t) + 2
t
$10^0$
$10^{-1}$
$10^{-1}$
$10^0$
$10^1$
$10^2$
$10^3$

FIG. 2.

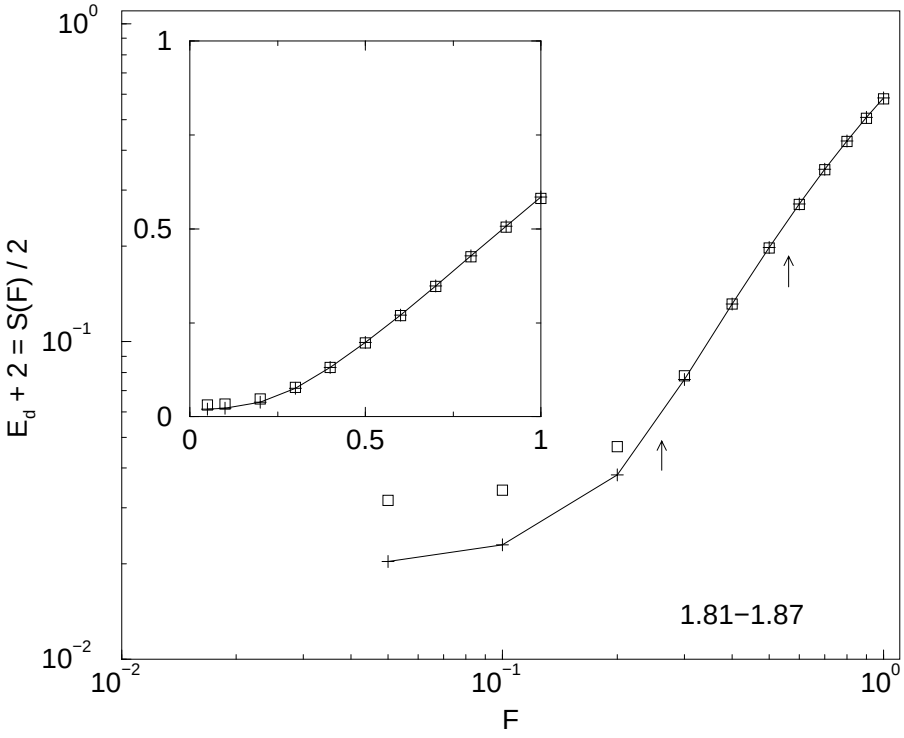
$10^0$
$10^{-1}$
$10^{-2}$
$E_d + 2 = S(F) / 2$
1
0.5
0
0
0.5
1
1.81−1.87
$10^{-2}$
$10^{-1}$
$10^0$
F

FIG. 3.

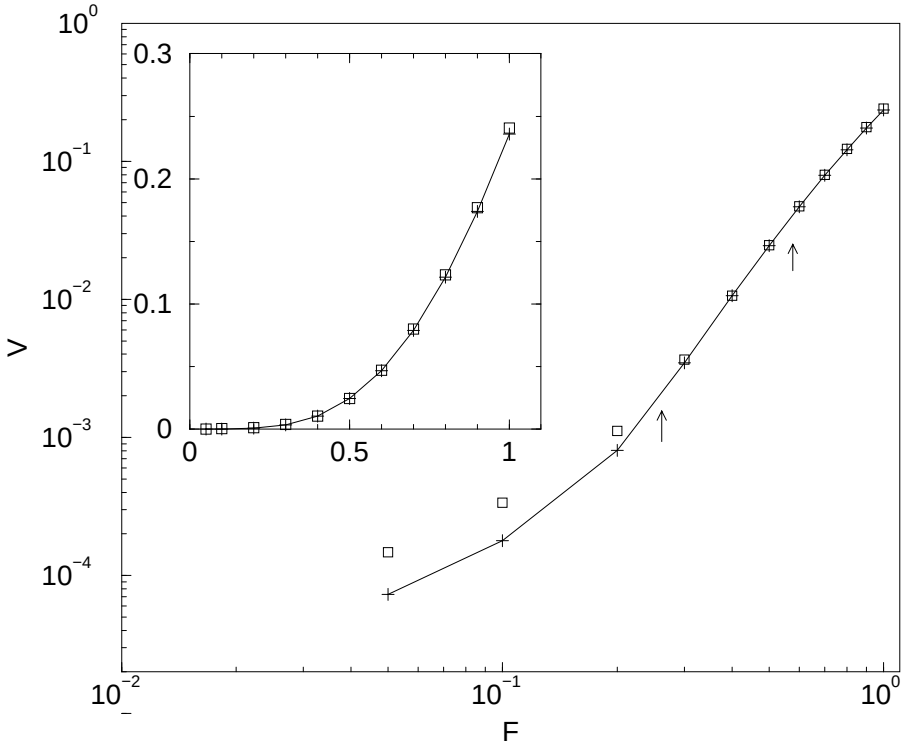
$10^0$
$10^{-1}$
$10^{-2}$
$10^{-3}$
$10^{-4}$
V
0.3
0.2
0.1
0
0
0.5
1
$10^{-2}$
$10^{-1}$
$10^0$
F

FIG. 4.

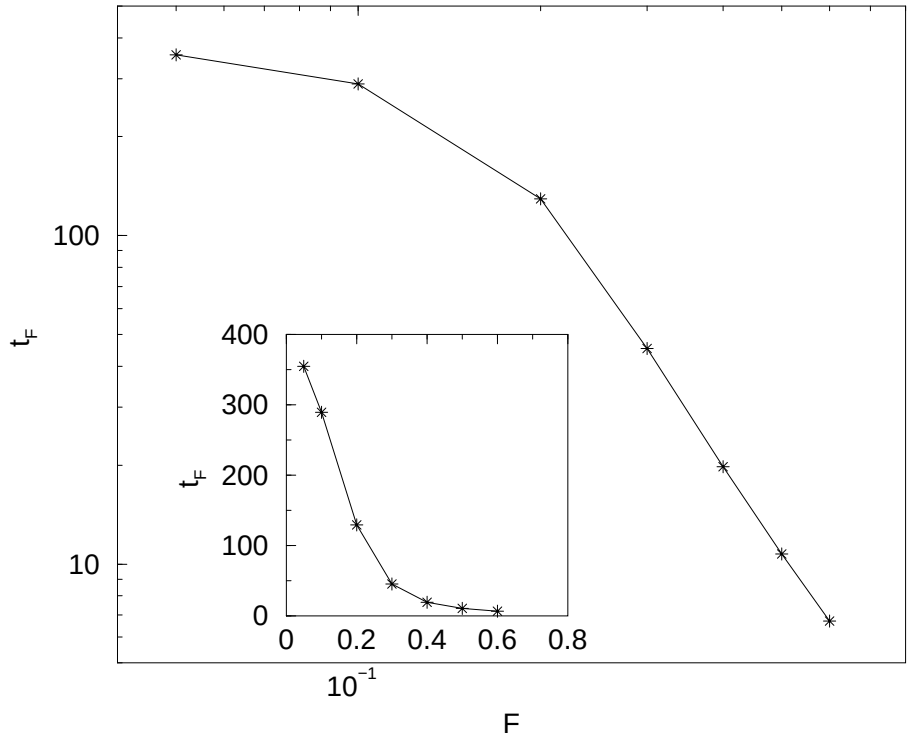
100
10
$t_F$
400
300
200
100
0
$t_F$
0
0.2
0.4
0.6
0.8
$10^{-1}$
F

FIG. 5.

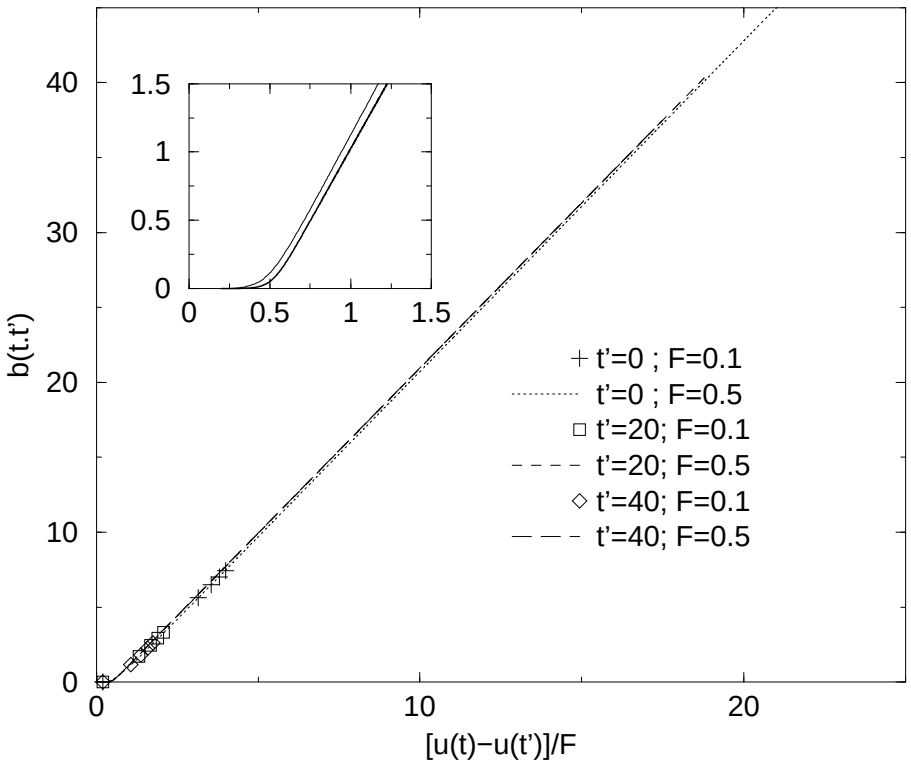
40
30
20
10
0
b(t,t')
1.5
1
0.5
0
0
0.5
1
1.5
0
10
20
[u(t)−u(t')]/F
t'=0 ; F=0.1
t'=0 ; F=0.5
t'=20; F=0.1
t'=20; F=0.5
t'=40; F=0.1
t'=40; F=0.5

FIG. 6.

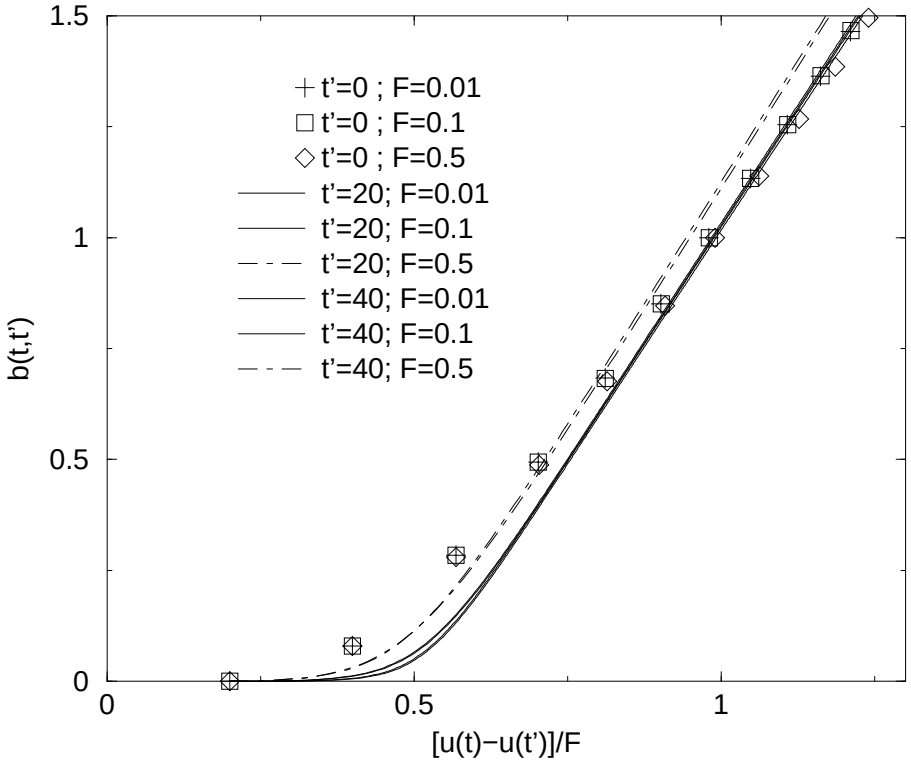
1.5
1
0.5
0
0
0.5
1
b(t,t')
[u(t)−u(t')]/F
t'=0 ; F=0.01
t'=0 ; F=0.1
t'=0 ; F=0.5
t'=20; F=0.01
t'=20; F=0.1
t'=20; F=0.5
t'=40; F=0.01
t'=40; F=0.1
t'=40; F=0.5

FIG. 7.